Electronic Supporting Information

A galvanic replacement reaction to synthesis of metal/ZnO heterostructured film on zinc substrate for enhanced photocatalytic performance

Kai Wang,[a,b] Zhangxian Chen,[a] Mengqiu Huang,[a] Zeheng Yang,[a] Chunyan Zeng,[a] Lei Wang,[a] Maoqin Qiu,[a] Yingmeng Zhang,[a] and Weixin Zhang,[a*]

a. School of Chemistry and Chemical Engineering, Hefei University of Technology
Hefei, 230009, Anhui, China, E-mail: wxzhang@hfut.edu.cn

b. School of Chemistry and Chemical Engineering, Beifang University of Nationality
Yinchuan, 750021, Ningxia, China

Figure S1

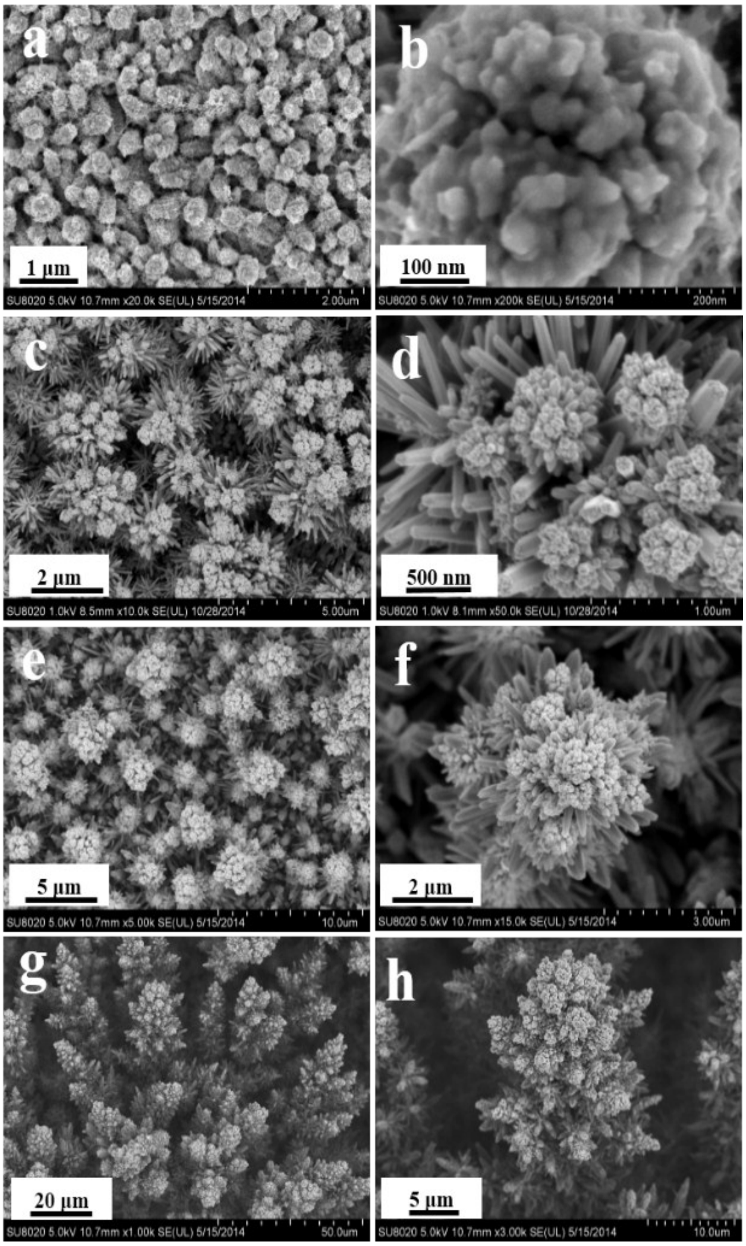

Figure S1. FESEM images of the as-obtained Cu/ZnO heterostructured film on zinc substrate at different reaction times: (a-b) 1 h, (c-d) 3 h, (e-f) 6 h, (g-h) 12 h.

Figure S2

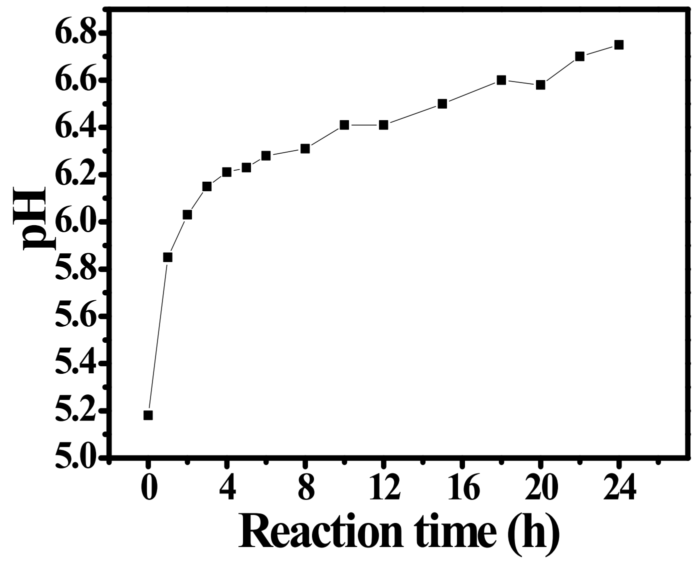

Fig. S2 The pH values of the reaction media as a function of reaction time during the synthesis of Cu/ZnO heterostructured films ($c_{(Cu2+)}$ = 0.6 mM).

Figure S3

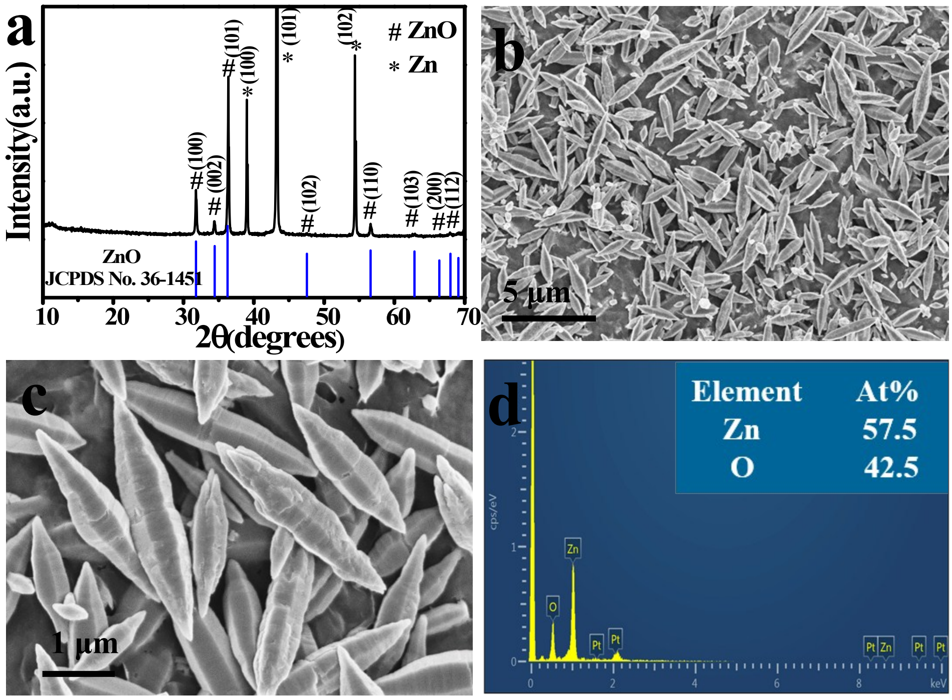

Fig. S3 (a) XRD pattern, (b, c) FESEM images and (d) EDS spectrum of the ZnO nanospindle films grown on zinc substrate.

Figure S4

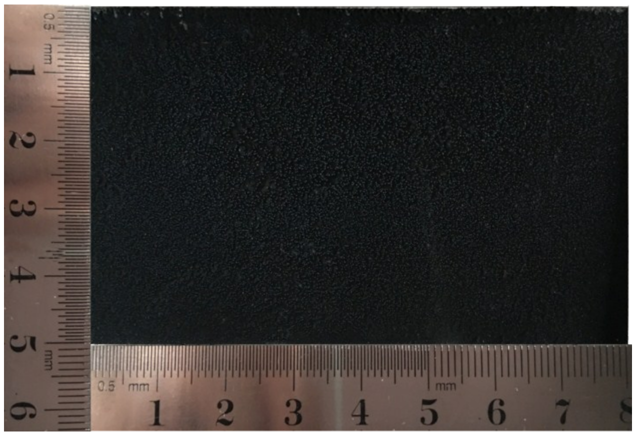

Fig. S4 The optical image of the Cu/ZnO hetrostructured film grown on large area of Zn substrate (40 cm^2).

Figure S5

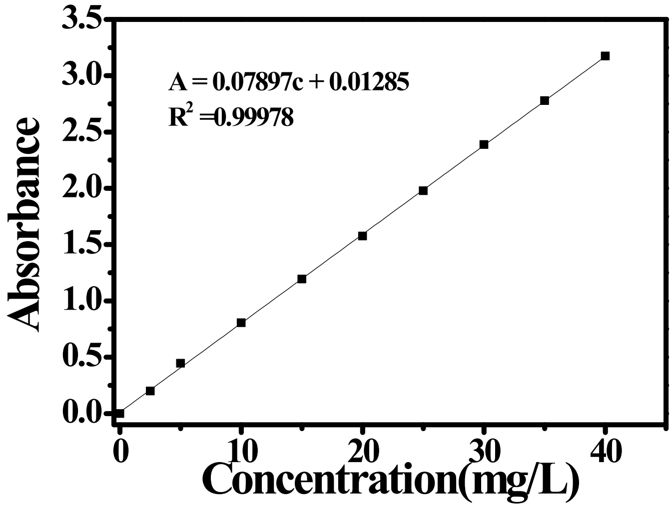

Fig. S5 The linear calibration curve for a series of standard MO aqueous solutions (0 mg/L, 2.5 mg/L, 5 mg/L,10 mg/L,15 mg/L, 20 mg/L, 25 mg/L, 30 mg/L, 35 mg/L and 40 mg/L).

Figure S6

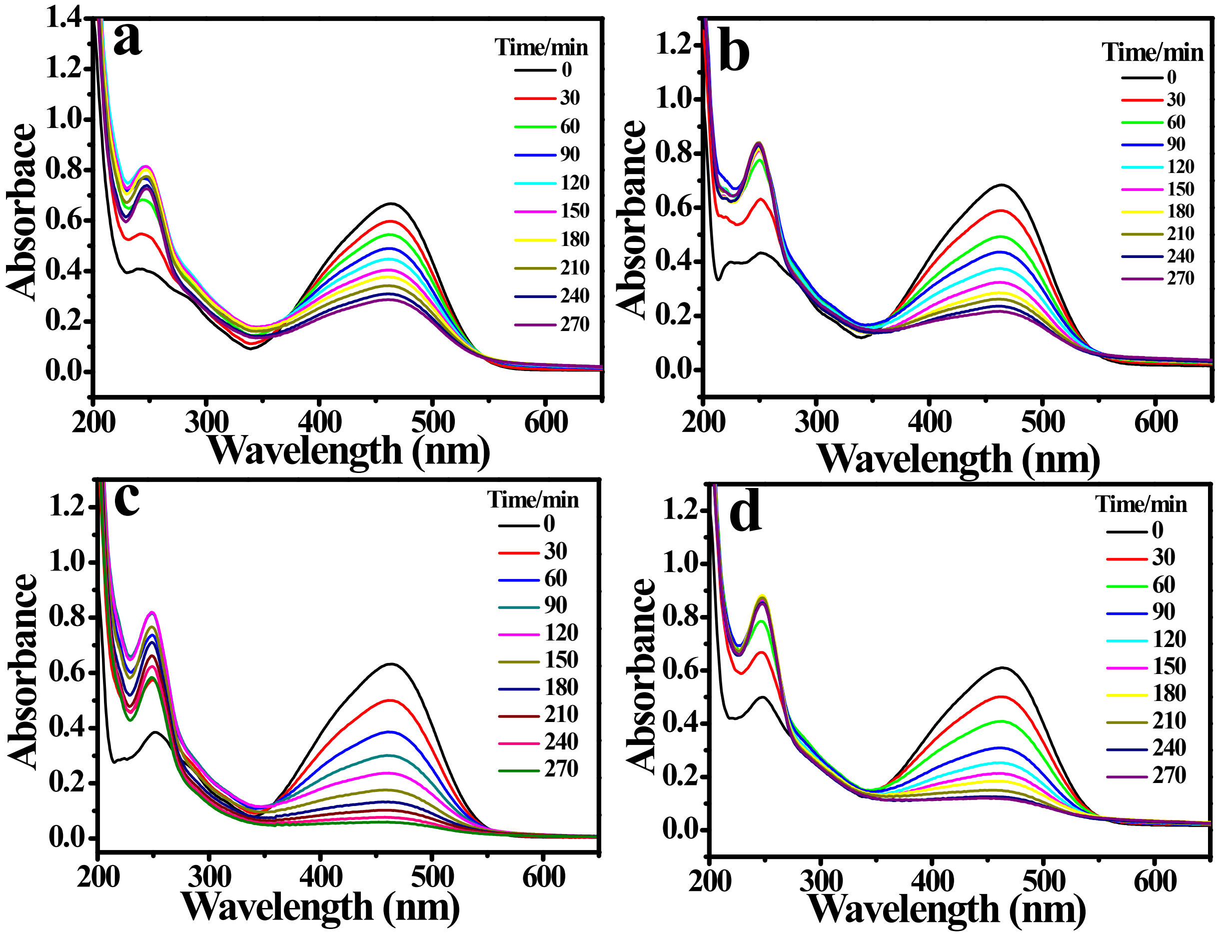

Fig. S6 Time-dependent UV-vis absorption spectra of MO aqueous solution under visible light irradiation in the presence of different photocatalysts: (a) ZnO, and Cu/ZnO heterostructures prepared with different concentrations of Cu^{2+}: (b) 0.2 mM (S1), (c) 0.6 mM (S2) and (d) 2.0 mM (S3).

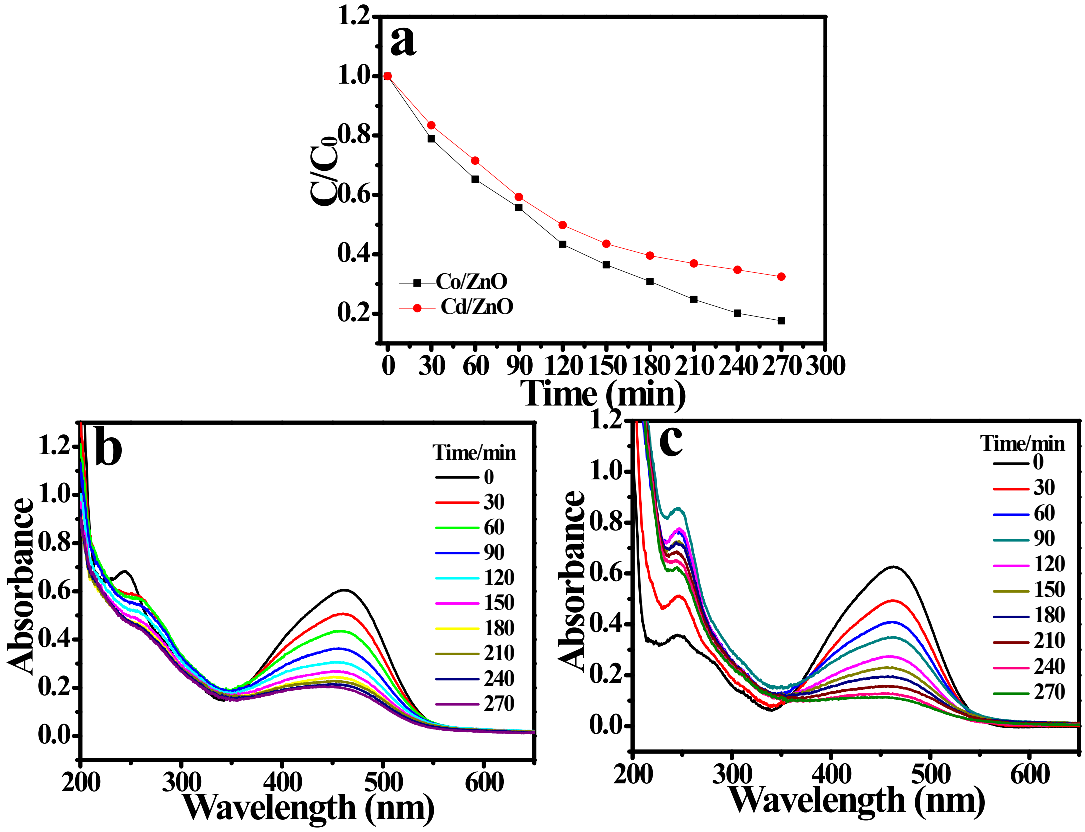

Fig. S7 (a) Photocatalytic degradation and (b, c) time-dependent UV-vis absorption spectra of MO solution with different catalysts: (b) Cd/ZnO and (c) Co/ZnO heterostructured films.

Figure S8

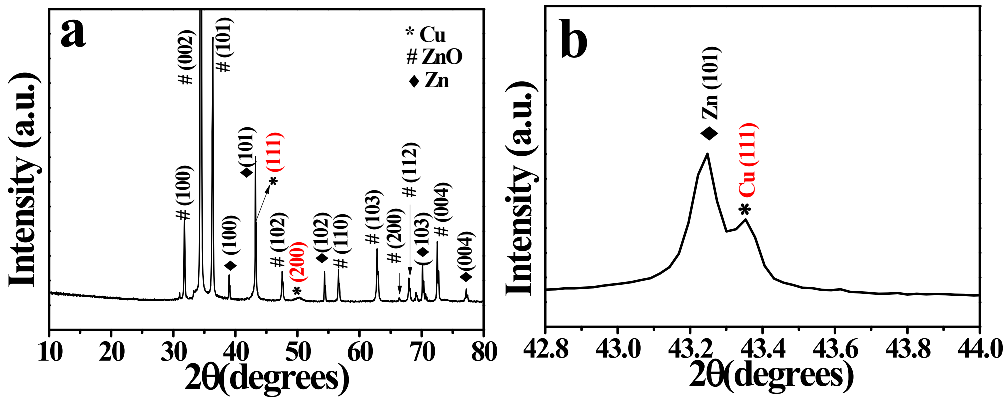

Fig. S8 (a) The XRD pattern of pine tree-like Cu/ZnO heterostructured film on zinc substrate after the fifth catalysis cycles. (b) Fine-scanned Zn(101) and Cu(111) peaks of the Fig.S8 a.

Fig. S8a presents the XRD pattern of pine tree-like Cu/ZnO heterostructured film on zinc substrate after the fifth catalysis cycles. It can be indexed to the cubic Cu (JCPDS No. 04-0836) and hexagonal wurtzite ZnO (JCPDS No. 36-1451). The peaks of Zn (JCPDS No. 04-0831) come from the zinc substrate. No other noticeable peaks from Cu_2O are observed, demonstrating the stability of the catalyst.

Figure S9

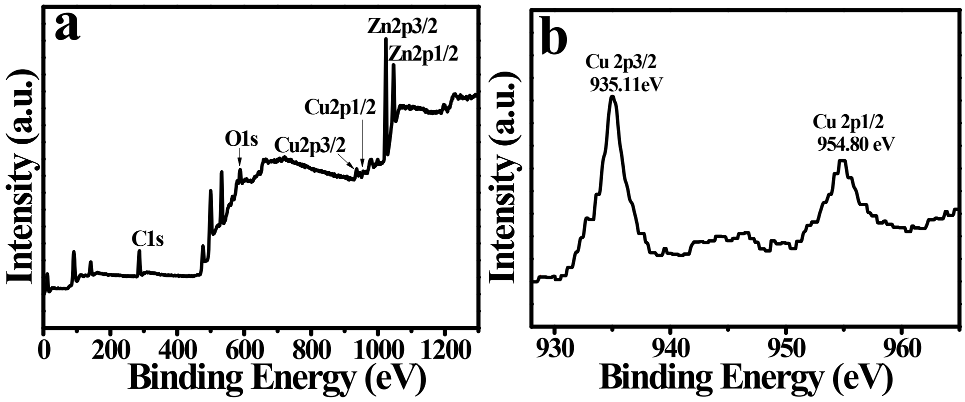

Fig. S9 XPS spectra of the pine tree-like Cu/ZnO heterostructured film on zinc substrate after the fifth catalysis cycles: (a) survey spectrum, and core-level spectra of (b) Cu 2p

To further evaluate the stability of the catalyst, the XPS survey spectrum (Fig. S9a) of the pine tree-like Cu/ZnO heterostructured film on zinc substrate after the fifth catalysis cycles indicates that in reference to the aliphatic C 1s peak (286.94 eV), elements of Cu, Zn and O can be detected. The binding energies of Cu 2p3/2 and Cu 2p1/2 are located at 935.11 eV and 954.80 eV, respectively (Fig. S9b), with a spin-orbital splitting of 19.69 eV. In addition, no obvious satellite peak can be observed after five cycles, suggesting that copper exists in zero valent in the Cu/ZnO heterostructured film.[15,16]

Figure S10

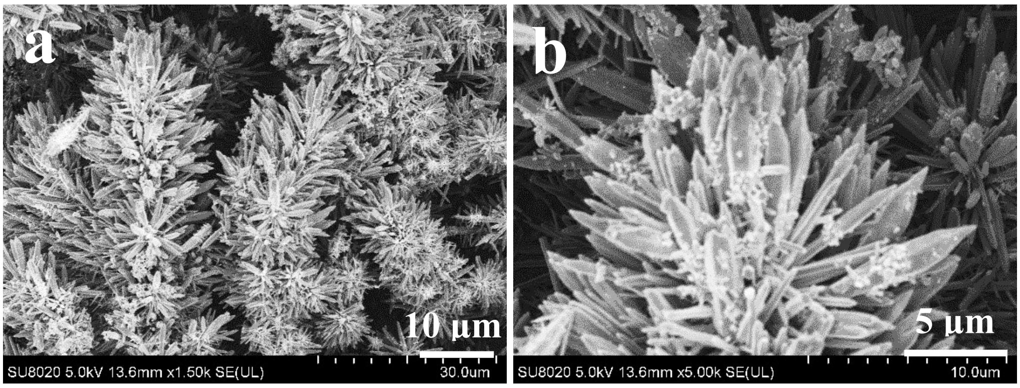

Fig. S10 (a) Low and high resolution FESEM images of pine tree-like Cu/ZnO heterostructured film on zinc substrate after the fifth catalysis cycles

Fig. S10 presents the FESEM images of pine tree-like Cu/ZnO heterostructured film on zinc substrate after the fifth catalysis cycles for the catalysis process of MO. After five cycles, the pine tree-like structure has deformed partly (Fig. S10a) but Cu nanoparticles can still be observed clearly on ZnO nanorods (Fig. S10b).

Figure S11

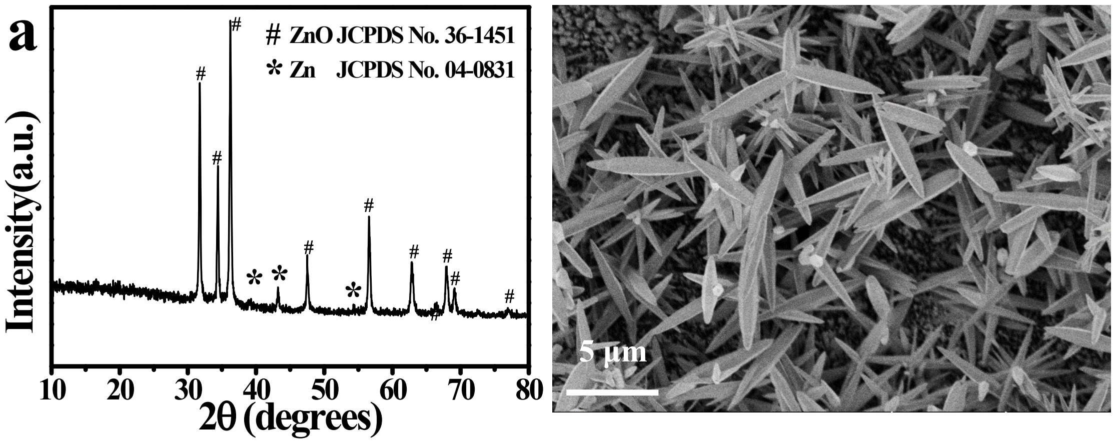

Fig. S11 (a) XRD pattern and (b) FESEM image of the bare ZnO nanospindle film on Zn substrate.

Synthesis of bare ZnO nanospindle film on Zn substrate: NaCl (0.0014 g) was mixed with 20.0 mL of deionized water and transferred into a 50 mL of Teflon-lined autoclave. The cleaned Zn substrate was placed horizontally in the autoclave and hydrothermally treated at 80 ^{o}C for 24 h. The milk-white samples were finally obtained.

The XRD pattern (Fig. S11a) can be indexed to the wurtzite ZnO (JCPDS No. 36-1451) and Zn (JCPDS No. 04-0831) from the substrate. The FESEM image (Fig. S11b) shows the ZnO nanospindles with lengths up to 5 μm and diameters around 500 nm.

Table S1. The cell phase and parameters of different substance

Substance	Crystal system	Cell parameters (Å)
ZnO	Hexagonal	a=b=3.24982, c=5.20661
Cu	Cubic	a=b=c=3.615
Co	Hexagonal	a=b=2.5031, c=4.0605
Cd	Hexagonal	a=b=2.9793, c=5.6181

Table S2. The standard electrode potentials (φ^{θ}) of different elements (25 ^{o}C)

Substance	Half-reaction	φ^{θ} (V)
Zn^{2+}/ Zn	Zn^{2+} + 2e = Zn	-0.76
Cu^{2+}/ Cu	Cu^{2+} + 2e = Cu	0.340
Cd^{2+}/ Cd	Cd^{2+} + 2e = Cd	-0.4025
Co^{2+}/ Co	Co^{2+} + 2e = Co	-0.277
Mg^{2+}/ Mg	Mg^{2+}+ 2e = Mg	-2.356